

# Lawrence Berkeley National Laboratory

## Recent Work

### Title

PAIR PRODUCTION IN THE FIELD OF ORBITAL ELECTRONS BY A TOTAL-ABSORPTION METHOD AT 300 MeV

### Permalink

<https://escholarship.org/uc/item/7gg0469w>

### Author

McDonald, Charles Alexander

### Publication Date

1954-06-02

UCRL 2595  
UNCLASSIFIED

UNIVERSITY OF  
CALIFORNIA

*Radiation  
Laboratory*

TWO-WEEK LOAN COPY

*This is a Library Circulating Copy  
which may be borrowed for two weeks.  
For a personal retention copy, call  
Tech. Info. Division, Ext. 5545*

BERKELEY, CALIFORNIA

## **DISCLAIMER**

This document was prepared as an account of work sponsored by the United States Government. While this document is believed to contain correct information, neither the United States Government nor any agency thereof, nor the Regents of the University of California, nor any of their employees, makes any warranty, express or implied, or assumes any legal responsibility for the accuracy, completeness, or usefulness of any information, apparatus, product, or process disclosed, or represents that its use would not infringe privately owned rights. Reference herein to any specific commercial product, process, or service by its trade name, trademark, manufacturer, or otherwise, does not necessarily constitute or imply its endorsement, recommendation, or favoring by the United States Government or any agency thereof, or the Regents of the University of California. The views and opinions of authors expressed herein do not necessarily state or reflect those of the United States Government or any agency thereof or the Regents of the University of California.

UCRL-2595  
Unclassified  
Physics

UNIVERSITY OF CALIFORNIA

Radiation Laboratory

Contract No. W-7405-eng-48

PAIR PRODUCTION IN THE FIELD OF ORBITAL ELECTRONS  
BY A TOTAL-ABSORPTION METHOD AT 300 MEV

Charles Alexander McDonald, Jr.

(Thesis)

June 2, 1954

Berkeley, California

PAIR PRODUCTION IN THE FIELD OF ORBITAL ELECTRONS  
BY A TOTAL-ABSORPTION METHOD AT 300 MEV

Table of Contents

	Abstract . . . . .	4
I.	Introduction . . . . .	5
II.	Absorption Processes at 300 Mev	
	A. Pair Production in the Nuclear Coulomb Field . . . . .	7
	B. Pair Production in the Coulomb Field of the Orbital Electrons, Triplet Production . . . . .	13
	C. Electron Compton Effect . . . . .	19
	D. Photomeson Production in Hydrogen and Carbon	
	1. Meson Production in Hydrogen. . . . .	19
	2. Meson Production in Carbon. . . . .	20
	E. Photostar Production. . . . .	21
	F. Photonucleon Reactions. . . . .	21
	G. Nuclear Photoeffect . . . . .	22
	H. Elastic Nuclear Scattering Processes . . . . .	22
	I. Photoelectric Effect . . . . .	22
III.	Method	
	A. Choice of Targets . . . . .	23
	B. Target Assembly . . . . .	25
	C. Total-Absorption Cross Sections . . . . .	25
IV.	Apparatus	
	A. Geometry . . . . .	29
	B. Pair Spectrometer and Vacuum System . . . . .	29
	C. Electron Detectors and Electronics . . . . .	31
	D. Beam Monitor . . . . .	31

V. Results and Conclusions	
A. Data . . . . .	36
B. Cross Sections . . . . .	36
Acknowledgments . . . . .	38
References . . . . .	39

PAIR PRODUCTION IN THE FIELD OF ORBITAL ELECTRONS  
BY A TOTAL-ABSORPTION METHOD AT 300 MEV

Charles Alexander McDonald, Jr.

Radiation Laboratory, Department of Physics  
University of California, Berkeley, California

June 2, 1954

ABSTRACT

The attenuation of 300-Mev photons in liquid hydrocarbons has been measured and has been used to infer the cross section for pair production in the field of the orbital electrons (triplet production).

Targets of benzene ( $C_6H_6$ ) and cyclohexane ( $C_6H_{12}$ ) were used in good geometry. A pair spectrometer with three fast counter channels was used to measure the attenuation of the beam. The synchrotron was monitored with a magnetic monitor which was susceptible only to the high-energy tail of the bremsstrahlung spectrum above 300 Mev.

The total absorption cross sections in hydrogen and carbon at 300 Mev have been found to be  $(1.88 \pm 0.10) \times 10^{-26}$  cm<sup>2</sup>/hydrogen atom, and  $(32.02 \pm 0.15) \times 10^{-26}$  cm<sup>2</sup>/carbon atom, respectively.

Subtraction of the theoretical nuclear pair and electron Compton cross sections and experimental photomeson cross sections in hydrogen from the total absorption cross section gives  $(0.75 \pm 0.11) \times 10^{-26}$  cm<sup>2</sup> for the experimental triplet cross section as compared with the theoretical value of  $0.786 \times 10^{-26}$  cm<sup>2</sup>. Similarly, when one subtracts the cross sections for competing processes in carbon, one gets for the triplet cross section at 300 Mev the value  $(4.70 \pm 0.62) \times 10^{-26}$  cm<sup>2</sup>, compared with the theoretical value of  $4.511 \times 10^{-26}$  cm<sup>2</sup>. The large uncertainty in the carbon triplet cross section is due to uncertainties in the cross sections for the competing processes.

PAIR PRODUCTION IN THE FIELD OF ORBITAL ELECTRONS  
BY A TOTAL-ABSORPTION METHOD AT 300 MEV

Charles Alexander McDonald, Jr.

Radiation Laboratory, Department of Physics  
University of California, Berkeley, California

June 2, 1954

INTRODUCTION

The possibility of the formation of a pair of electrons in the field of the orbital electrons of an atom by a gamma ray was first recognized by Perrin.<sup>1</sup> Landau and Rumer,<sup>2</sup> for the reciprocal case of bremsstrahlung by an electron in the field of orbital electrons, suggested that one should replace  $Z^2$  by  $Z(Z + 1)$  in order to account for the total radiation cross section per atom. The first quantum mechanical calculation of the process was that of Wheeler and Lamb.<sup>3</sup> They used the first Born approximation, which assumes that  $Z/137 \ll 1$ , included screening, and found that screening with less effective on the electrons than it was on the nucleus. Thus, so-called "triplet production" (pair production in the field of the orbital electrons) is greater than  $\Phi_{\text{Pair}}/Z$ . This is discussed in more detail later (section IIB). Several nonscreened theories have been given, the most complete being that of Borsellino.<sup>4</sup> He finds that pair production in the field of an electron very slowly approaches that in the field of a nucleus of unit charge. At 300 Mev the former is 5% smaller than the latter.

The first indisputable observation of triplet production was that reported in 1944 by Ogle and Kruger,<sup>5</sup> who used the 2.67-Mev gamma from radiosodium. This is just above the threshold ( $4mc^2$ ) for triplet production, and -- as has been shown by Watson<sup>6</sup> and more rigorously by Vortruba<sup>7</sup> -- the three electrons tend to share the available energy about equally for a photon energy that is less than 5 Mev; while for photon energies above this, the positron and one electron get most of the energy with the third electron getting  $1/2 mc^2$  in the extreme relativistic limit. Thus, to observe the effect directly, one should use



gammas just above the threshold. Ogle and Kruger observed the pairs and triplets formed in the air in their cloud chamber. They detected 56 pairs and 2 triplets with excellent momentum and energy balance. More recent cloud-chamber work was that by Phillips and Kruger<sup>8</sup> with the 6-Mev gamma from protons on fluorine, by Gaertner and Yeater<sup>9</sup> with the average energy of 50 Mev from the General Electric betatron, and by Emigh<sup>10</sup> at the Illinois 300-Mev betatron. Besides these direct observations, DeWire<sup>11</sup> at 280 Mev, Lawson<sup>12</sup> at 88 Mev, and Berman<sup>13</sup> at 19.5 Mev have all found it necessary to introduce the theoretical absorption by triplet production to account for the total absorption experimentally observed. However, only Berman studied low-Z elements, where triplet production is comparable to pair production, and his energy was too low to give rise to a pair cross section comparable to Compton cross section.

Since triplet production is one of the basic interactions between radiation and matter, it was proposed to carry out an experiment in which the cross section for this process would be determined to statistically significant accuracy. As was mentioned above, at high energies one of the electrons gets very little energy. Thus, a total-absorption experiment was chosen as the best method of detecting the process.

## II. ABSORPTION PROCESSES AT 300 MEV

### A. Pair Production in the Nuclear Coulomb Field

For 300-Mev gamma rays, the largest contribution to the total absorption cross section in all elements except hydrogen is that due to pair production in the nuclear Coulomb field. The theory for this process, including screening, was given by Bethe and Heitler<sup>14</sup> in 1934. They used the Dirac negative energy states and the first Born approximation, which requires that  $Z/137 \ll 1$ , this being the requirement that the plane wave representation used for the pair members remain undistorted by the nuclear Coulomb field. For high-Z elements the condition is not satisfied. This was first seen experimentally by Lawson<sup>12</sup> at 88 Mev, who found

$$\Phi_{\text{Theory}} \approx \Phi_{\text{Pair}} (1 + 2 \times 10^{-5} Z^2)$$

was a good approximation. This discrepancy with theory has since been confirmed by several authors, among them DeWire, Ashkin and Beach<sup>15</sup> at 280 Mev, and Emigh<sup>10</sup> who gets at 300 Mev substantially the same correction as that found by Lawson. The differential cross section in the limit of high energies but neglecting screening has been calculated without recourse to the Born approximation by Maximon and Bethe<sup>16</sup> and has recently been integrated over positron energy.<sup>17</sup> It is shown in reference 17 that the correction is equally applicable to cases with complete, incomplete, or no screening. Just as the experiments had indicated, the correction term has a  $Z^2$  dependence. It is to be noted that this correction is completely negligible for carbon, amounting to less than 0.1%, and for elements of lower Z. As is shown below, triplet production is most readily detectable for low-Z elements. Thus we are justified in calculating nuclear pair production from the Bethe-Heitler theory, in view of its experimental confirmation for low Z.

In calculating the screening of the nucleus by the orbital electrons, a Fermi-Thomas distribution of the electrons<sup>18</sup> is assumed. This theory is of a statistical nature and is more applicable as the Z becomes higher. Fortunately, Wheeler and Lamb<sup>3</sup> have made an exact calculation for hydrogen.

A convenient form for the differential cross section,  $\bar{\Phi}_P(E_+) dE_+$ , for the creation of a pair whose positron has an energy in the range  $E_+$  to  $E_+ + dE_+$ , whose negative electron has an energy in the range  $E_-$  to  $E_- + dE_-$ , and for the incident quantum whose energy is  $k_0$ , where  $k_0 = E_+ + E_-$ , is given by the relation

$$\bar{\Phi}_P(E_+) dE_+ = \frac{\bar{\Phi} dE_+}{k_0^3} \left\{ \left[ E_+^2 + E_-^2 \right] \left[ \phi_1(\gamma) - \frac{4}{3} \ln Z \right] + \frac{2}{3} E_+ E_- \left[ \phi_2(\gamma) - \frac{4}{3} \ln Z \right] \right\},$$

where  $\phi_1(\gamma)$  and  $\phi_2(\gamma)$  are given graphically in Fig. 1 as functions of

$$\gamma = \frac{100 mc^2 k_0}{E_+ E_- Z^{1/3}}$$

and where

$$\bar{\Phi} = \frac{Z^2}{137} \left( \frac{e^2}{mc^2} \right)^2 = Z^2 \times 5.793 \times 10^{-28} \text{ cm}^2. \text{ In the case of}$$

hydrogen, one gets  $\phi_1(\gamma)$  and  $\phi_2(\gamma)$  from Wheeler and Lamb<sup>3</sup> (see Fig. 1).

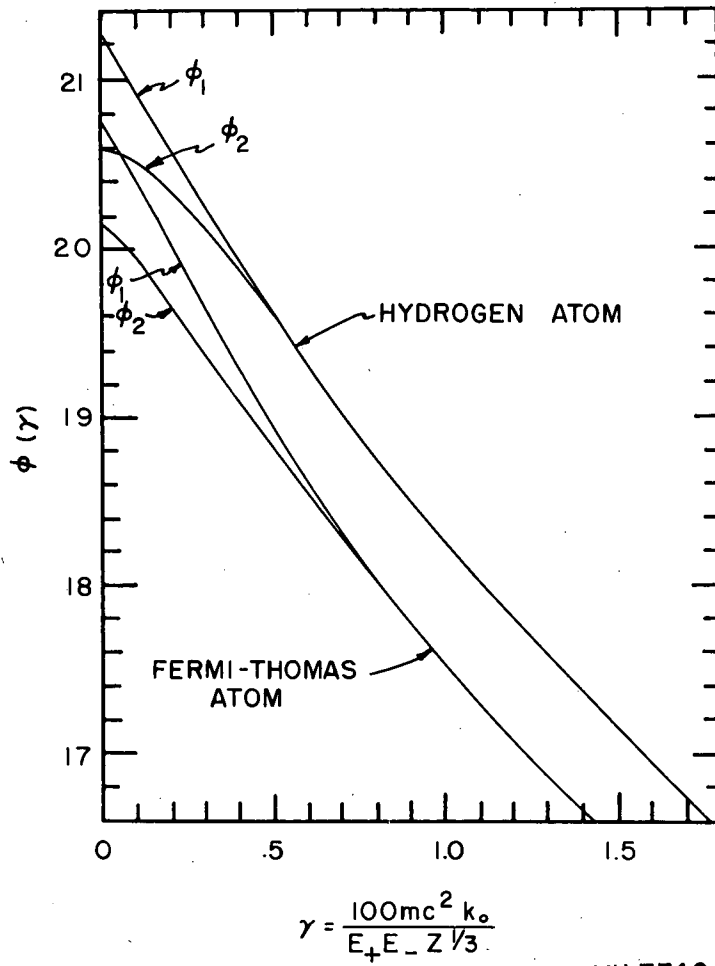


Fig. 1  
Plot of  $\phi_1(\gamma)$  and  $\phi_2(\gamma)$  vs  $\gamma = \frac{100 mc^2 k_0}{E_+ E_- Z^{1/3}}$  for the Bethe-Heitler  
pair production theory.<sup>3</sup>

The author has calculated the value of this function for  $k_0 = 300$  Mev for hydrogen and carbon as a function of the positron total energy. A curve of the points is shown in Fig. 2, and a comparison to the triplet cross section is shown later in Fig. 6. The maximum interval between points was 10 Mev. The total pair cross sections were obtained by graphical integration of these curves (see Table 1 below). From calculations such as this, a plot of the pair cross section vs. photon energy may be obtained. Such a curve is shown in Fig. 3.

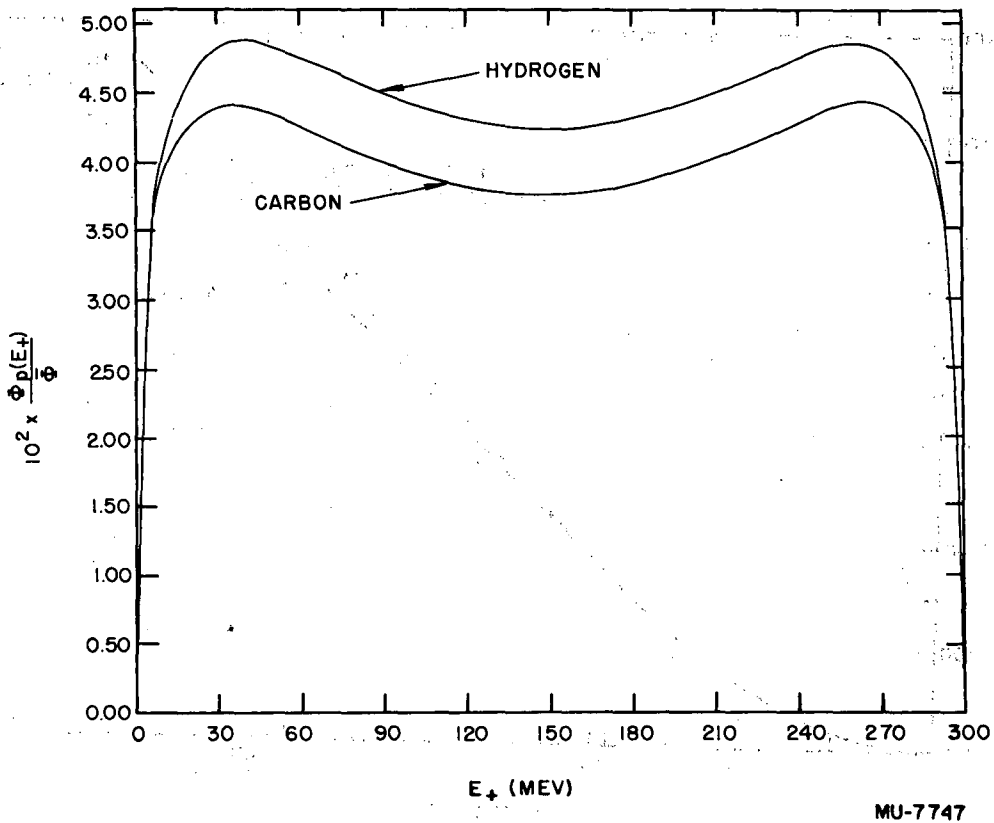


Fig. 2  
Plot of  $\bar{\Phi}_p(E_+)$ , the differential pair-production cross section  
by the Bethe-Heitler theory, vs  $E_+$ , the positron total energy, for  
 $k_0 = 300$  Mev. Hydrogen and carbon curves are plotted in units of

$$\bar{\Phi} = \frac{Z^2 \left( \frac{e^2}{mc^2} \right)^2}{137}$$

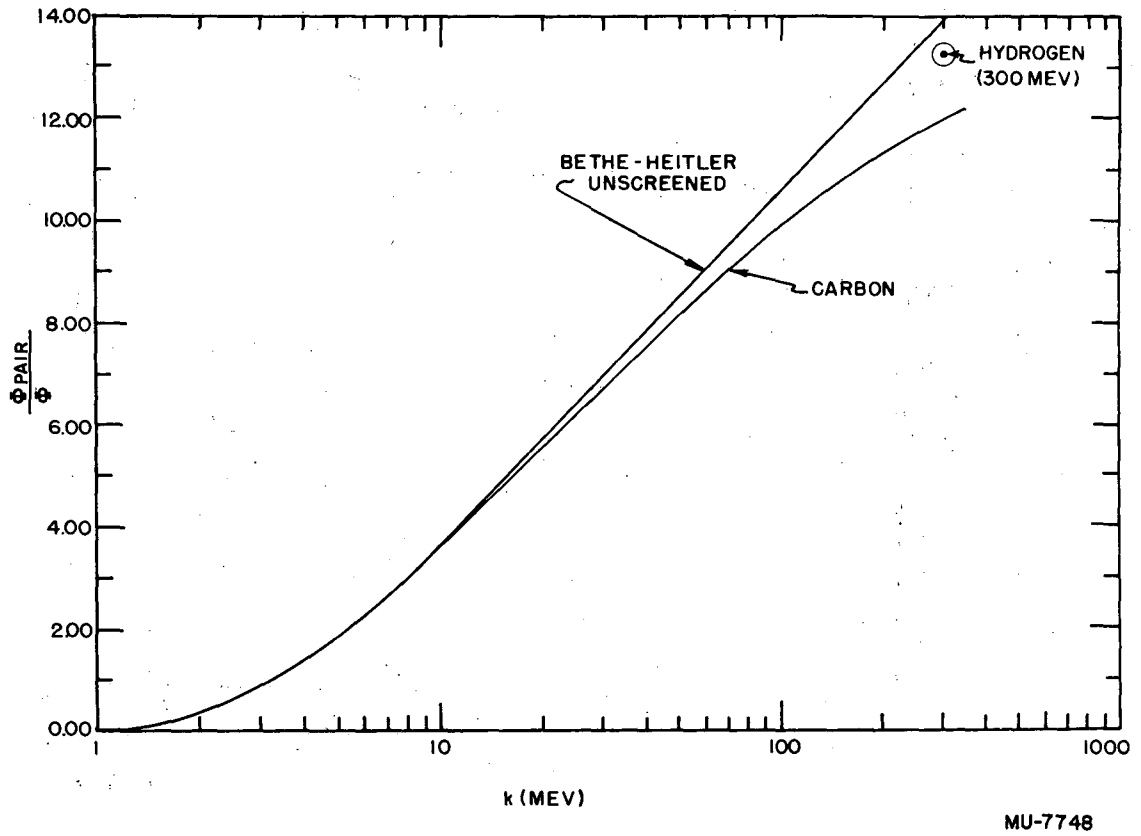


Fig. 3  
Pair-production cross section vs. photon energy.

MU-7748

B. Pair Production in the Coulomb Field of the Orbital Electrons,  
Triplet Production

A process of absorption for 300-Mev gamma rays which is second in magnitude only to pair production is that of triplet production. The name is derived from the fact that the quantum forms a pair of electrons in the field of an orbital electron, and the electron recoils and is removed from the atom, giving a triplet of electrons. An elementary calculation shows that the threshold for the process is  $4 mc^2$ , where it is  $2 mc^2$  in the case of ordinary nuclear pair production.

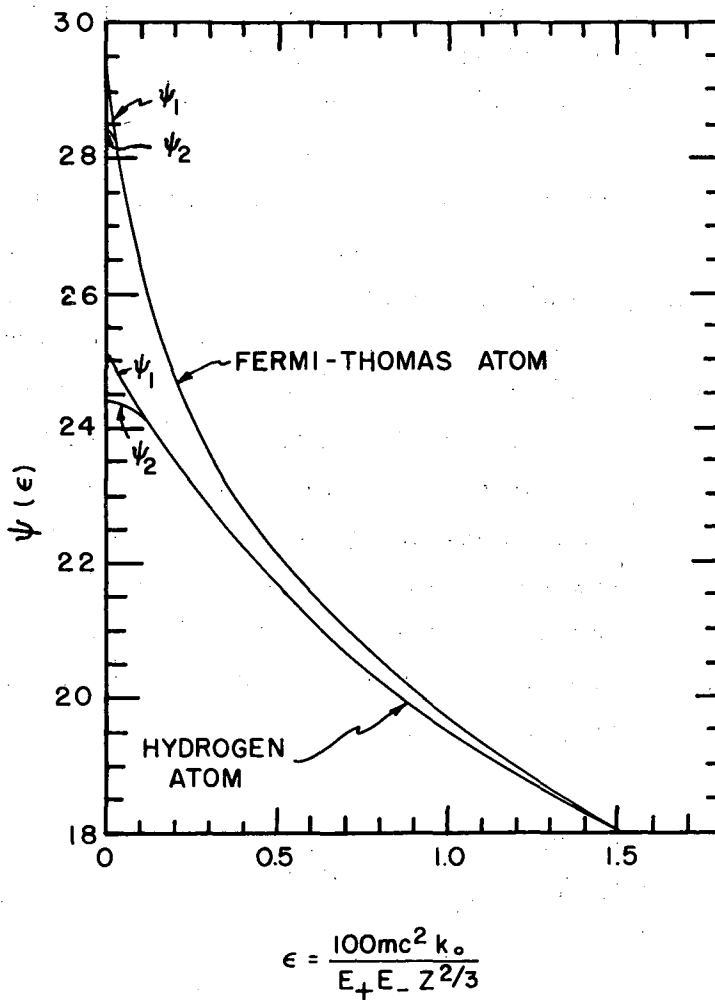
The article by Wheeler and Lamb<sup>3</sup> is primarily devoted to pair production by electrons in the field of orbital electrons, but by the Weizsacker-Williams method<sup>19</sup> they obtain the result for triplet production. The calculation closely follows that of Bethe and Heitler for ordinary pair production. They employ the first-order Born approximation, which assumes a plane-wave representation for the pair members. They also assume that the recoil energy of the third electron is negligible, an assumption which has remained in more recent theories and has been shown to be valid by Watson<sup>6</sup> and Votruba.<sup>7</sup> For screening, the Fermi-Thomas electron distribution is again assumed, except in the case of hydrogen, where exact wave functions were used. The differential cross section for the production of a pair of electrons in the field of an orbital electron in which the positron has an energy in the interval  $E_+$  to  $E_+ + dE_+$ , and for the incident quantum of energy  $k_0$ , is given by

$$\Phi_t(E_+) dE_+ = \frac{4\pi\alpha^2}{Z} \frac{dE_+}{k_0^3} \left\{ \left[ E_+^2 + E_-^2 \right] \left[ \psi_1(\epsilon) - \frac{8}{3} \ln Z \right] + \frac{2}{3} E_+ E_- \left[ \psi_2(\epsilon) - \frac{8}{3} \ln Z \right] \right\},$$

where  $\psi_1(\epsilon)$  and  $\psi_2(\epsilon)$  are given graphically in Fig. 4 as functions of

$$\epsilon = \frac{100 mc^2 k_0}{E_+ E_- Z^{2/3}}.$$





MU-7749

Fig. 4  
 Plot of  $\psi_1(\epsilon)$  and  $\psi_2(\epsilon)$  vs  $\epsilon = \frac{100 mc^2 k_0}{E_+ E_- Z^{2/3}}$  for the Wheeler-Lamb  
 triplet production theory.<sup>3</sup>

For H and C the plot of this equation as a function of the positron total energy ( $E_+$ ) is given for  $k_0 = 300$  Mev in Fig. 5, points having been taken at least every 10 Mev. A comparison to pair production is given in Fig. 6. The total triplet cross sections for hydrogen and carbon were obtained by graphical integration of these curves. The results of these calculations are given in Table I below. It is to be noted that screening is less effective on the orbital electrons than it is on the nucleus. In the limit of very high energies and complete screening we find

$$\frac{Z \bar{\Phi}_{WL}}{\bar{\Phi}_{BH}} = 1.4 \text{ in hydrogen. }^{20}$$

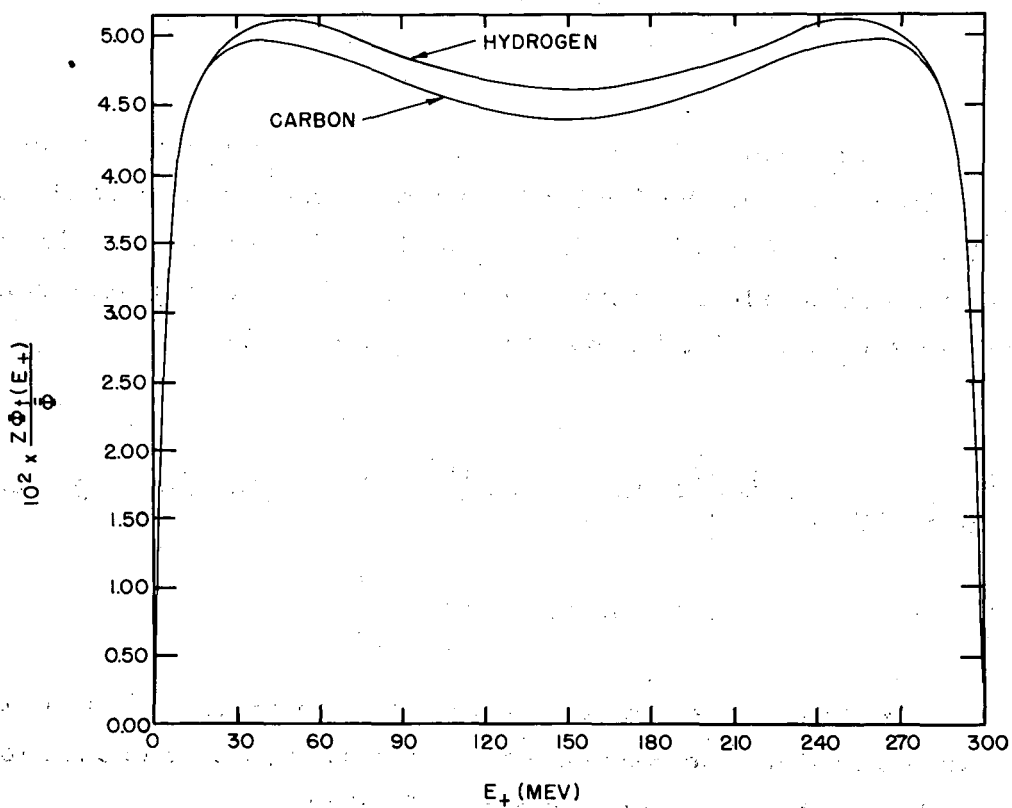
In this derivation, Wheeler and Lamb have assumed that the probability of producing a pair in the Coulomb field of a free electron is the same as that of a proton. Borsellino<sup>4</sup> has shown that this assumption is not correct but he has neglected screening. In the limit of high energies, Borsellino's result for the total triplet cross section per atom is

$$\begin{aligned} \bar{\Phi}_t)_{\text{Borsellino}} = \frac{\bar{\Phi}}{Z} \left[ \frac{28}{9} \ln 2a - \frac{218}{27} - \frac{1}{a} \left\{ \frac{4}{3} (\ln 2a)^3 - 3(\ln 2a)^2 \right. \right. \\ \left. \left. + 6.84 \ln 2a + 21.51 \right\} \right] \end{aligned}$$

where  $a = k_0/mc^2$ . As one goes to very high energies this result has as its asymptotic limit the Bethe-Heitler nonscreened pair-production cross section divided by the atomic number. That is

$$\bar{\Phi}_t)_{\text{Borsellino}} \rightarrow \frac{\bar{\Phi}}{Z} \left[ \frac{28}{9} \ln 2a - \frac{218}{27} \right] \text{ for } a \gg 1.$$

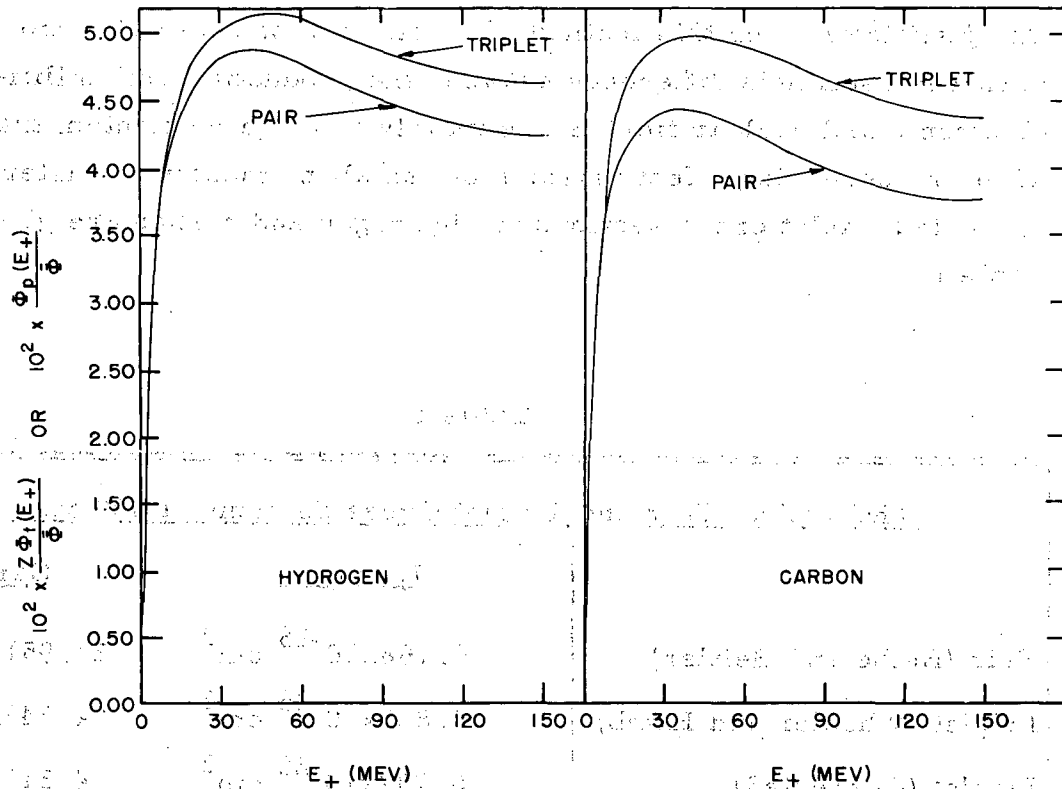
Borsellino's result approaches this function very slowly, differing from it by 5% at 300 Mev.



MU-7750

Fig. 5  
Plot of  $\Phi_t(E_+)$ , the differential triplet-production cross section for the Wheeler-Lamb theory, vs  $E_+$ , the positron total energy, for  $k_0 = 300$  Mev. Hydrogen and carbon curves are plotted in units of  $\frac{\Phi_t}{Z}$ .

... ..  
... ..  
... ..  
... ..  
... ..  
... ..



MU-7751

Fig. 6  
(a) Comparison of hydrogen pair and triplet differential cross sections.  
(b) Comparison of carbon pair and triplet differential cross sections.

At the intermediate energy of 300 Mev it is necessary to consider both screening and the difference between electronic and nuclear effects. Bethe and Ashkin<sup>20</sup> point out that it is a good approximation to take Borsellino's result for the difference between the cross sections in the field of an electron and in the field of a nucleus of charge 1, and to subtract this from the Wheeler and Lamb cross section. That is:

$$\Phi_{\text{triplet}} = \Phi_{\text{t W.L.}} - Z \left[ \Phi_{\text{Pair (Z=1) unscreened B.H.}} - \Phi_{\text{triplet (Z=1) Borsellino}} \right]$$

The justification for this method of calculation of the triplet cross section is that Borsellino's difference between the production probabilities for electronic and nuclear field is due mainly to large momentum transfers, while the screening effect arises from small momentum transfers. The corrected triplet cross sections for hydrogen and carbon are given in Table I.

Table I

<u>Theoretical Pair and Triplet Cross Sections at 300 Mev</u>		
	<u>Hydrogen</u>	<u>Carbon</u>
Pair (Bethe and Heitler)	0.768x10 <sup>-26</sup> cm <sup>2</sup>	24.951x10 <sup>-26</sup> cm <sup>2</sup>
Triplet (Wheeler and Lamb)	0.825x10 <sup>-26</sup> cm <sup>2</sup>	4.743x10 <sup>-26</sup> cm <sup>2</sup>
Triplet (Corrected)	0.787x10 <sup>-26</sup> cm <sup>2</sup>	4.511x10 <sup>-26</sup> cm <sup>2</sup>

### C. Electron Compton Effect

An absorption process in which the energy of the photon is degraded is Compton scattering. Here the incident photon interacts with an orbital electron of an atom, raising that electron to the continuum, with the quantum being scattered at reduced energy. The quantum-mechanical derivation of the process was given by Klein and Nishina.<sup>21</sup> They employed the Dirac electron theory and obtained a result that has been verified experimentally at energies up to 300 Mev.

By means of a total-absorption experiment on beryllium, in which the pair production processes are eliminated by determining the ratio of Be and Pb pair cross sections, Kenney<sup>22</sup> has verified the Compton cross section to within 10% at 300 Mev, where his major uncertainties are in the photomeson and photostar cross sections, discussed below in this section. Coensgen<sup>23</sup> has found a 17% discrepancy with the theory at 253 Mev in his angular distribution of the scattered photons, but he points out that this is possibly due to errors in the energy calibration of the synchrotron.

Thus one is justified in taking for the Compton effect the Klein-Nishina formula for the total scattering cross section per electron:

$$\Phi_C = \frac{3 \phi_0}{8 a} \left\{ \left[ 1 - \frac{2(a+1)}{a^2} \right] \ln(2a+1) + \frac{1}{2} + \frac{4}{a} - \frac{1}{2(2a+1)^2} \right\}$$

where  $a = k_0/mc^2$  and  $\phi_0 = \frac{8\pi}{3} \left( \frac{e^2}{mc^2} \right)^2$ . At 300 Mev,  $\Phi_C = 3.21 \times 10^{-27} \text{ cm}^2/\text{electron}$ .

### D. Photomeson Production in Hydrogen and Carbon

#### 1. Meson Production in Hydrogen

The element that has been the most thoroughly investigated with regard to photomeson production is hydrogen. Interest has centered on hydrogen, owing to the relative simplicity of the interaction, for which there is some hope for a theoretical explanation. Since the case of photon on

nucleon giving meson plus nucleon represents the only true two-body problem in photomeson production, this is the only case in which the energy of the incident gamma is determined completely by the meson angle and energy, and hence the only one in which we are entirely free of the added complication of using meson cross sections given in terms of equivalent quanta.

Energy and angular distributions for  $\pi^+$ -meson production in hydrogen have been measured at various laboratories. The recent Berkeley total cross section at 275 Mev<sup>24</sup> is in excellent agreement with that from California Institute of Technology.<sup>25</sup> Unpublished data from the latter institution gives for the total  $\pi^+$  production cross section in hydrogen at 300 Mev the value:

$$\sigma_H(\pi^+, 300 \text{ Mev}) = 2.2 \times 10^{-28} \text{ cm}^2$$

Data on  $\pi^0$  production at 300 Mev in hydrogen are available for the point at  $90^\circ$  to the beam in the laboratory system.<sup>26</sup> As yet, the angular distribution is in enough doubt to warrant assuming that the distribution is similar to that for  $\pi^+$  production. The total  $\pi^0$  cross section was obtained by multiplying the differential cross section at  $90^\circ$  by the ratio of the total  $\pi^+$  cross section at 300 Mev to the differential  $\pi^+$  cross section at 300 Mev at  $90^\circ$  to the beam. This gave

$$\sigma_H(\pi^0, 300 \text{ Mev}) = 2.3 \times 10^{-28} \text{ cm}^2$$

Thus the total  $\pi$ -meson cross section in hydrogen at 300 Mev is  $0.045 \times 10^{-26} \text{ cm}^2$ . This result should be good to 50%.

## 2. Meson Production in Carbon

The photoproduction of  $\pi^+$ ,  $\pi^-$ , and  $\pi^0$  has been observed in carbon. The interpretation of the results is complicated by the fact that the cross sections are quoted in terms of equivalent quanta. Because of this, one must be very cautious in the uncertainty one attributes to the cross section when the conversion is made from equivalent quanta to cross section per photon at a particular energy.

The ratio of  $\pi^+$  production from carbon and from hydrogen per equivalent quantum is given as 2.16 by Jakobson, Shultz, and White.<sup>27</sup> Using this result and the  $\pi^+$  cross section in hydrogen at 300 Mev,<sup>25</sup> gives

$$\sigma_C (\pi^+, 300 \text{ Mev}) = 4.7 \times 10^{-28} \text{ cm}^2$$

The ratio of  $\pi^-$  to  $\pi^+$  production in carbon at 265 Mev was found by Carothers<sup>28</sup> to be 1.27, with no strong energy or angular dependence. Combining this with the  $\pi^+$  cross section stated above gives

$$\sigma_C (\pi^-, 300 \text{ Mev}) = 6.0 \times 10^{-28} \text{ cm}^2$$

In the paper by Steinberger, Panofsky, and Steller<sup>29</sup> the ratio of the cross sections per equivalent quanta for  $\pi^0$  production in carbon and in hydrogen is 7.7. From the hydrogen cross section one gets

$$\sigma_C (\pi^0, 300 \text{ Mev}) = 17.7 \times 10^{-28} \text{ cm}^2$$

Thus the total photomeson cross section in carbon at 300 Mev is  $0.28 \times 10^{-26} \text{ cm}^2$ . This result should be good to within a factor of two.

#### E. Photostar Production

The photoproduction of three or more pronged stars in carbon has been observed by Miller.<sup>30</sup> In the interval of 242 to 322 Mev, the average value for the total cross section is given as  $1.5 \times 10^{-27} \text{ cm}^2$ , where an additional 10% was added to account for stars in which only neutrons were formed. This cross section should be good to within 50%.

#### F. Photonucleon Reactions

Photonucleon reactions give rise to a single strong resonance in their excitation functions in the vicinity of 20 Mev. At energies very far above this resonance, the cross section would be expected to be negligibly small, less than  $10^{-32} \text{ cm}^2$  at 300 Mev in carbon. Terwilliger and Jones<sup>31</sup> have reported a rise in the  $(\gamma, n)$  cross sections above the



photomeson threshold giving a cross section of about  $10^{-27}$  cm<sup>2</sup>/carbon atom at 300 Mev. It seems reasonable to interpret this increase as being due to photostar production in which a meson is created and reabsorbed. If this is the case, the cross section for this effect has already been included in that for photostar production.

#### G. Nuclear Photoeffect

Levinthal and Silverman<sup>32</sup> have studied the electromagnetic ejection of fast protons from carbon and found that the cross section at 300 Mev is about  $10^{-28}$  cm<sup>2</sup> within a factor of 10. The process here is of the type described by Chew and Goldberger.<sup>33</sup> The more recent data of Keck<sup>34</sup> indicate that the cross section is of this same order of magnitude, but some discrepancy exists in the absolute value of the cross section.

#### H. Elastic Nuclear Scattering Processes

Elastic nuclear scattering processes such as Thomson scattering from the nucleus as a whole, nuclear resonance scattering, etc., contribute a total cross section at 300 Mev in carbon of  $10^{-30}$  cm<sup>2</sup>, which is entirely negligible.

#### I. Photoelectric Effect

The photoelectric effect, which is so important as a mechanism for gamma-ray absorption at lower energies, is negligible at 300 Mev, and is included here merely for the sake of comparison and to complete the list. Heitler<sup>35</sup> gives the following cross section for the effect at energies far from an absorption edge:

$$\phi_K = \frac{3}{Z} \frac{Z^5}{137^4} \frac{\phi_0}{\gamma}$$

$$\text{where } \phi_0 = \frac{8\pi}{3} \left( \frac{e^2}{mc^2} \right)^2 = 6.651 \times 10^{-25} \text{ cm}^2$$

$$\text{and } \gamma = k_0 / mc^2$$

Thus, for hydrogen at 300 Mev,  $\phi_K)_{H, 300 \text{ Mev}} = 2.42 \times 10^{-36} \text{ cm}^2$ ,

where there is only one K-shell electron. For carbon, one gets  $4.48 \times 10^{-32} \text{ cm}^2$ , where a factor of 5/4 was included to take care of the photoeffect from the other electron shells.<sup>36</sup>

### III. METHOD

The most direct method of obtaining the triplet cross section would be to detect the three electrons for a given photon energy. It has been mentioned previously that the third electron gets very little of the energy at 300 Mev. Thus the direct observation of the effect, either electronically or by cloud chambers, would be exceedingly difficult if not impossible. Superimposed upon this difficulty is the problem of working with a bremsstrahlung spectrum.

A simpler approach is to measure the total absorption cross section for a given photon energy for elements in which the triplet cross section is an appreciable fraction of that total absorption cross section. If, from theory and experiment, one can make reasonable estimates of the cross sections for the competing processes at this energy, a value of the triplet cross section can be obtained.

#### A. Choice of Targets

It is desirable to have the triplet cross section as large as possible with respect to the nuclear pair cross section. Since the former has a  $Z$  and the latter a  $Z^2$  dependence, one would naturally choose as small a  $Z$  as is practical. Hydrogen is the obvious choice, since at 300 Mev the two effects are about equal in magnitude, each contributing about 40% of the total absorption cross section, with the Compton effect giving 18% and photomeson production the remainder. Unfortunately, hydrogen in gas or liquid form is difficult to work with, and the attenuation due to the hydrogen would be very small with existing targets.

One could go to other elements in liquid or solid form, but the hydrocarbons, benzene ( $C_6H_6$ ) and cyclohexane ( $C_6H_{12}$ ), have some definite advantages that ultimately led to their being selected. They are readily available in high-purity samples. They are free of the fire, explosion, and general handling problems inherent in hydrogen targets, while having a hydrogen concentration comparable to that of liquid hydrogen. Unfortunately, their use requires a subtraction type of experiment. However, one also obtains the total absorption cross section in carbon at the same time. Due to the prodigious number of counts necessary to give reasonable accuracy on the hydrogen cross section in a subtraction type of experiment, the carbon cross section, which is about 15 times as large, will have been determined to the best accuracy obtainable. This will have been accomplished with an absorber whose density is known to within a few parts in  $10^4$ . These hydrocarbons make it possible to determine the total absorption cross section in carbon to a much higher precision than would be possible with a graphite target, owing to the density uncertainties in the latter.

From the total absorption cross section in carbon, one can also determine the triplet cross section. It is true that carbon lacks the simplicity of hydrogen, in which the number of possible processes is very limited, but the competing reactions in carbon (other than nuclear pair, triplet and Compton effect) still amount to less than 2 percent of the total. At the same time, the triplet effect contributes about 12 percent. Thus one has the possibility of measuring the triplet cross section to even higher accuracy than is possible with hydrogen. Owing to screening, which is a function of the atomic number, this will not be simply six times the cross section of hydrogen. It is thus seen that this subtraction experiment has proven itself valuable.

## B. Target Assembly

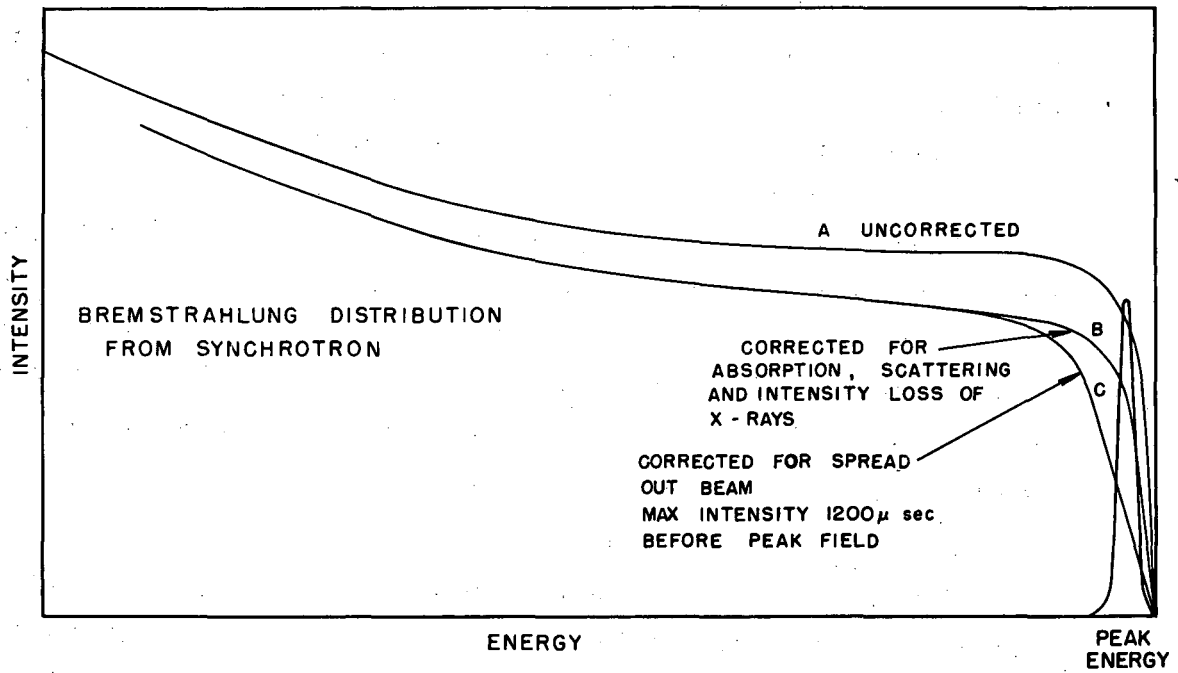
The two hydrocarbons were contained in identical aluminum cylinders, 29 inches long and 2-1/2 inches in diameter, with 5-mil aluminum end windows. The absorber length was chosen so as to give approximately  $1/e$  attenuation of the gamma-ray beam at 300 Mev. The temperature of the targets was monitored, and the data were corrected for density variation and change in target length.

Since the method of the experiment was to measure the ratio of the number of 300-Mev quanta that penetrate the absorber to the number reaching that point with no absorber, it was necessary to have a third target. This one was identical with the other two except that it was evacuated to less than 15 microns. This provides a true measure of the target-out condition, and eliminates the necessity of subtracting out the absorption due to the Al windows and also correcting for the displaced air column.

The three targets were placed in a "trapeze" target changer, which was remotely controlled from the counting area. This device insured the alignment of the targets with respect to the beam and also allowed one to cycle targets often without necessitating trips into the magnet room. This point is discussed in greater detail below (see section V A).

## C. Total Absorption Cross Sections

To measure the total absorption cross sections in hydrogen and carbon, it was necessary to determine the ratio of the number of 300-Mev quanta that reach the converter of the pair spectrometer when the absorber is in place to the number reaching that point without the absorber. The latter measurement is made with the evacuated dummy target in place of the hydrocarbon target. The pair spectrometer was equipped with three channels of coincidence apparatus (described in detail below; here it is considered only as an instrument for determining the intensity of photons at the energy  $k$  and with a resolving power shown in Fig. 7).<sup>37</sup>



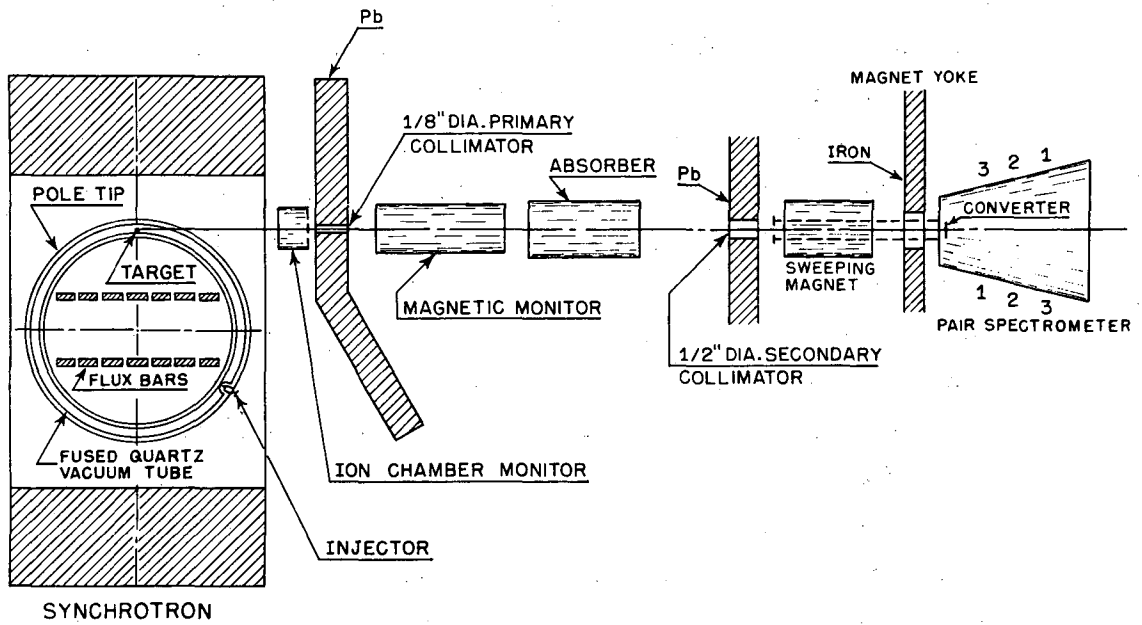
MU3198

Fig. 7  
Bremsstrahlung spectrum and pair spectrometer resolving power plotted in arbitrary units. 41

With this equipment it is possible to determine for each of the hydrocarbons a number closely related to the total absorption coefficient at the energy  $k$ . Of course these values are averaged over the resolution of the spectrometer.

The choice of the energy  $k$  is based on several considerations arising from the use of a bremsstrahlung continuum spectrum, Fig. 7. The primary problem in a total absorption experiment is to maintain the requisites for good geometry. This means that if the incident particle has any interaction whatsoever with any atom in the target, then it must be completely removed from the beam. With photons, all processes are one-shot affairs, that is to say, the quantum is completely absorbed when it interacts with matter. The situation is actually more complicated than this for two reasons. First, one can have Compton scattering in which the photon energy is degraded to some smaller value; and second, there can be cascade or shower processes in the absorber, which degrade the photon energy. Owing to relativistic transformation of space, the shower particles are concentrated in the forward or beam direction. Thus attenuation at the energy  $k$  does occur, but if one is operating too far below the maximum synchrotron energy  $k_0 = 335$  Mev, one also counts degraded photons from the energy interval between  $k$  and  $k_0$  that happen to fall within the acceptance band of the spectrometer.

To reduce this possibility as far as possible, the absorber was placed as far from the geometry-defining collimator before the spectrometer as space would permit (see Fig. 8). The maximum solid angle subtended by the 1/2-inch collimator at the absorber was  $10^{-3}$  steradian. Next, the spectrometer was set to detect an energy of approximately 90% of  $k_0$ . This energy gives a negligibly small possibility for degraded photons, while providing a sufficient number of primary quanta to make the experiment feasible. The value finally chosen was  $k = 300$  Mev.



MU-6875

Fig. 8  
Schematic arrangement of apparatus.

#### IV. APPARATUS

##### A. Geometry

The general experimental setup is shown in Fig. 8. The circulating electron beam in the synchrotron strikes a 20-mil platinum target producing a bremsstrahlung spectrum. The rf envelope is shaped so as to spread out the beam over 3000 to 4000 microseconds.

The gamma-ray beam, after emerging from the quartz doughnut, passed through a thin-walled ion chamber, which in the past had served as the monitor for the synchrotron beam (about which more is said below). At a distance of 55 inches from the Pt target the beam was collimated to 1/8 inch by a brass-lined primary collimator in a lead wall 9 inches thick. Next was a 1/4-inch collimator in a 6-inch lead wall, to remove the electron spray produced by the primary collimation.

The beam next passed through the magnetic monitor, discussed below, and finally struck the absorber. After the absorber was the final collimator. It was a 1/2-inch-diameter hole in a 6-inch-thick lead wall. This collimator served to remove the shower particles that were outside the beam core, the beam diameter there being 3/8 inch.

All collimators, targets and converters were aligned with the beam with a telescope which was positioned photographically. The position of each of these was checked photographically before each run and again at the end of the run.

##### B. Pair Spectrometer Magnet and Vacuum System

After passing through the tertiary collimator, the beam enters the vacuum chamber through a lucite port. This section of the vacuum chamber is built in the 2-3/4-inch gap of a shielded sweeping magnet. The field in the gap is 8 kilogauss and extends over 30 inches of beam path, removing all charged particles from the beam.

This clean beam, in vacuum, then enters the pair-spectrometer magnet. In the 5-1/2-inch gap of this magnet a vacuum chamber has been constructed around a set of trapezoidal pole tips. The best vacuum attained was 300 microns, but this was more than sufficient to remove the necessity for correcting for the conversion in the air column between the



sweep magnet and the pair spectrometer. With the sweep magnet but without the vacuum chamber the intervening air column was about  $3 \times 10^{-3}$  radiation lengths, and gave an appreciable electron background. With sweep magnet and vacuum chamber no coincidence counts were recorded when the converter was removed from the beam. This vacuum chamber was designed by Dr. R. W. Kenney.

The pair-spectrometer magnet current was electronically regulated and was controlled remotely from the counting area. Its value was observed on a Leeds and Northrup potentiometer in the counting area, the signal originating from a 50-millivolt 200-ampere shunt.

The magnetic field in the pair magnet was normally run at 8.5 kgauss. A detailed plot of the field with these pole tips had been made previously<sup>37</sup> with search coil and magnetometer apparatus. An absolute magnetization curve was run, using proton moment equipment. The latter test was rerun for the present experiment, since a different shunt had been used in the earlier experiment. The estimated accuracy of the field over the electron trajectories is 0.3%, and the field uniformity varies by less than 0.5% from pole tip center to electron detector and converter positions.

The electron detectors, three along each side of the pair magnet, were placed along a straight line making a  $30^\circ$  angle with the beam axis and passing through the center of the converter. In this way, in the extreme relativistic limit, the detector distance from the converter is directly proportional to the electron energy acceptable at the detector. The center detector on each side, position 2 in Fig. 8, was rigidly fixed, its position having been calculated from the absolute field data. The other four detectors were movable over short distances. Positions 1-1, 2-2 and 3-3 each form a coincidence counting channel. These three channels were set to the same energy, 300 Mev, by the following method: The experimental shape of the bremsstrahlung spectrum near its quantum limit was determined by varying the magnetic field in the pair magnet. The shapes given by the three channels are not expected to be exactly the same, owing to differences in counter efficiencies, etc. The cutoffs

must be the same, however, if all channels are really set to look at the same energy. The movable counters were repositioned and the curves were again run until all three cutoffs coincided. The spectrometer was then set to look at 300-Mev quanta with a channel width of 6 Mev.

### C. Electron Detectors and Electronics

The photons were converted in a Pb or Be converter, its position being remotely controlled. The pair electrons were detected in stilbene scintillation crystals 1 by 1/2 by 1/2 inch in size. These were mounted on 3-foot lucite light pipes, which were viewed by 1P21 photomultiplier tubes. The 1P21's were magnetically shielded and watercooled to reduce noise.

The phototube output pulse was first limited and then clipped to  $1.5 \times 10^{-9}$  seconds, and the two signals for each channel were then fed into bridge-type coincidence circuits. The bridge output was amplified and sent to the counting area for further amplification and then scaled. A block diagram is shown in Fig. 9. A typical resolving-time curve is shown in Fig. 10. Accidentals were checked with  $2 \times 10^{-8}$ -second delay in one side of the bridge, and the ratio of accidentals to reals was maintained at less than 0.5%. These counters and electronics were designed and built by Dr. R. W. Kenney, with the coincidence circuit closely following that designed by Dr. Lee Neher.<sup>38</sup>

### D. Beam Monitor

At the Berkeley synchrotron, as well as at other electron synchrotrons and betatrons, it has been common practice to monitor the bremsstrahlung beam with ionization chambers. The so-called "precollimator Nunan ionization chamber" at the synchrotron has thin aluminum walls. It has its maximum sensitivity to approximately 6-Mev quanta, and over 90% of its response is due to quanta of less than 200 Mev when the quantum limit of the bremsstrahlung is 335 Mev. Thus, the contribution of the upper 10% of the bremsstrahlung (300-335 Mev) to the total ion-chamber output is so small (less than 2%) that if the quantum limit fluctuated slightly, giving large changes in the number of photons in this energy interval, it would not be detectable. The shifts in the quantum limit are

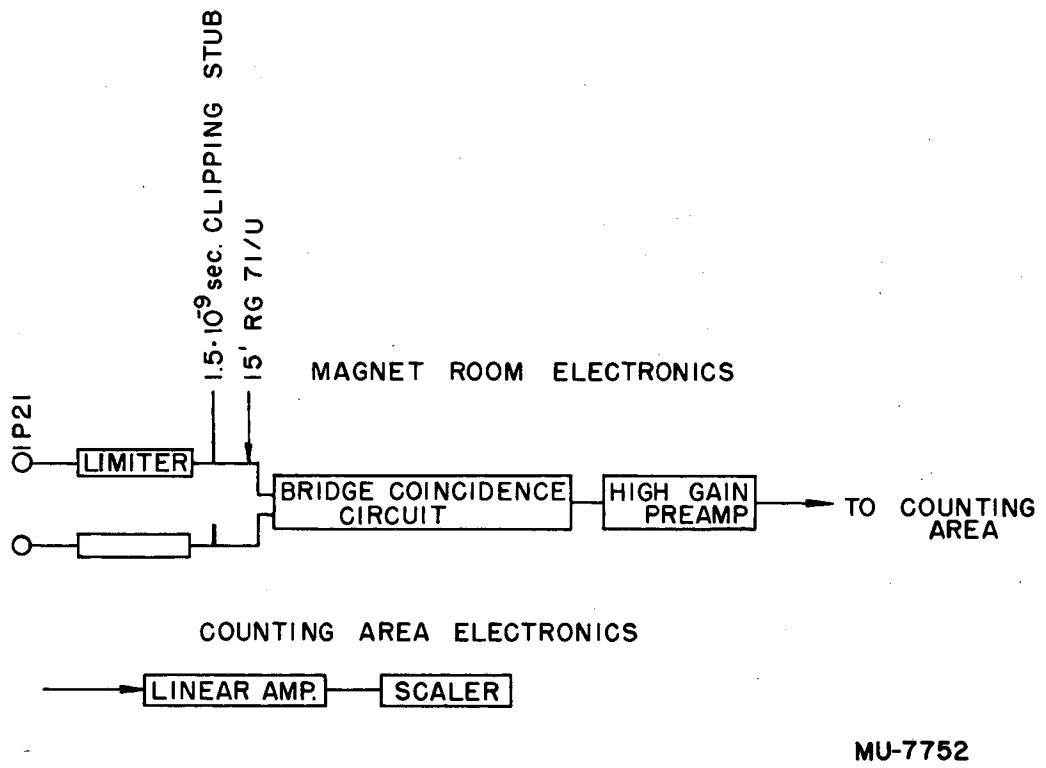
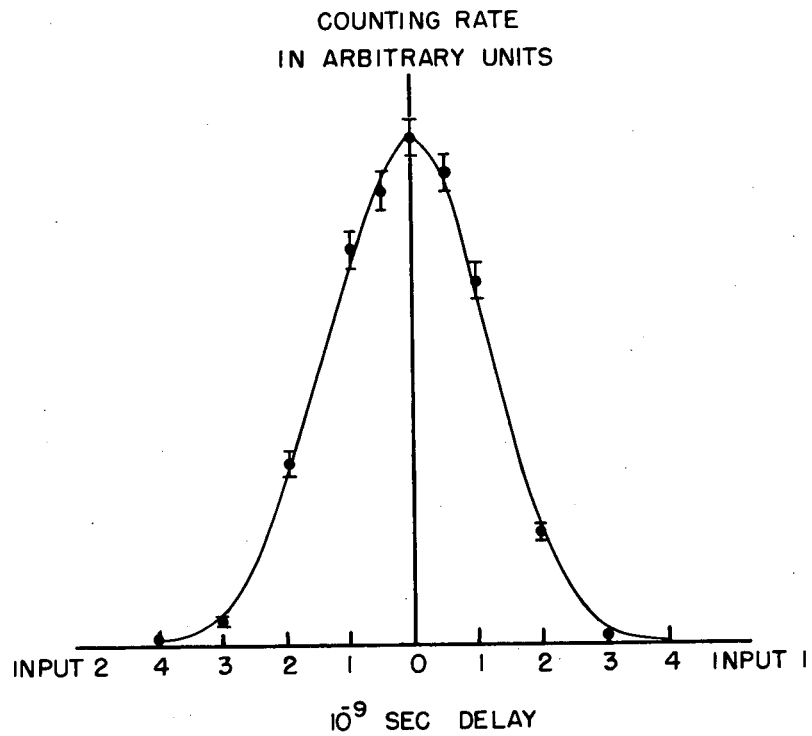


Fig. 9  
Block diagram of electronics for one coincidence channel.



MU 3203

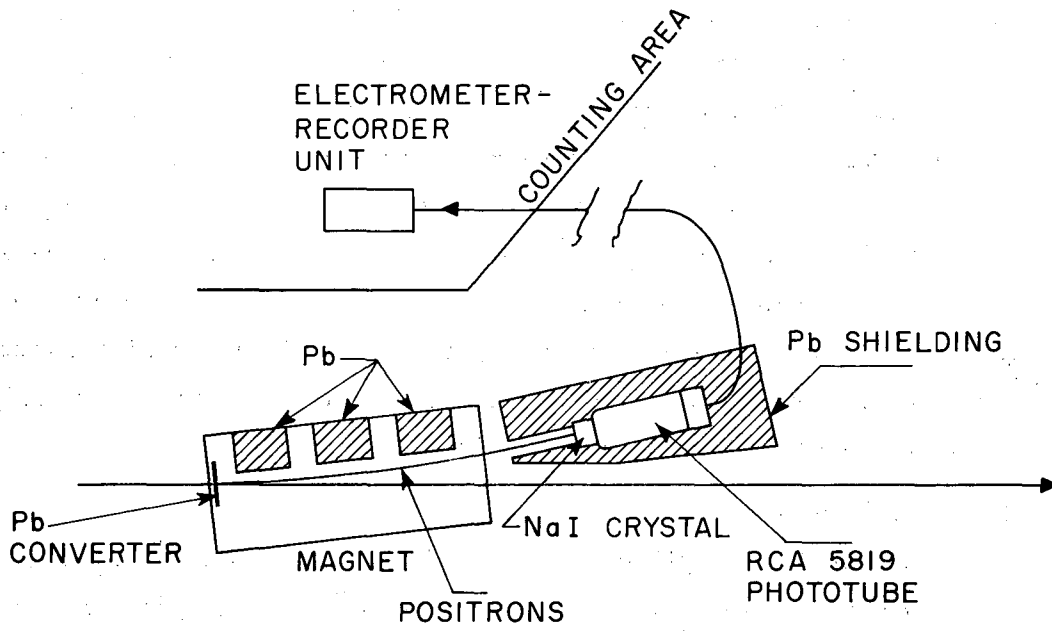
Fig. 10  
Typical resolving-time curve of bridge coincidence circuits  
using  $1.5 \times 10^{-9}$ -sec input pulses from 300-Mev electron pairs.  
Counting rate in arbitrary units.

primarily due to variations in the capacitor high voltage and in the shape of the rf envelope (which determines the time with respect to peak field and the energy of the electrons when they strike the synchrotron target). It is thus seen that an ionization chamber is a poor monitor for bremsstrahlung flux when one operates near the spectrum cutoff. This was first observed experimentally when a single-channel pair spectrometer looking at 300-Mev quanta was used directly in the synchrotron beam. It was found that the number of coincidence counts per unit of integrated flux as measured by the ion chamber varied by 15%.

Consequently, any attempt to operate near the cutoff of the bremsstrahlung, as one must do in the present experiment to reduce the possibility of counting degraded photons (see section III C), would be susceptible to a very large error in monitoring. A magnetic monitor<sup>39</sup> was set up, in which positrons from a thin lead converter are analyzed by a magnetic field (see Fig. 11). The field of 5 kgauss was provided by a small sweep magnet to deflect positrons of  $300 \pm 10$  Mev into a narrow momentum channel. The positrons were detected by a sodium iodide crystal, which was well shielded from the main gamma-ray beam and was viewed by a 5819 photomultiplier. The phototube was magnetically shielded and was water-cooled to reduce dark current. The output current of this tube was integrated on a condenser and recorded by an electrometer circuit in the counting area, from which the relative beam flux in the energy interval from 300 to 335 Mev could be read. The instantaneous photomultiplier current was 3 orders of magnitude smaller than the rated maximum current.

This monitor was checked against the pair spectrometer with coincidence channels set to look at pairs from 300-Mev quanta. Machine parameters of the synchrotron were varied over allowable limits, and the magnetic monitor tracked the pair spectrometer within counting-rate statistics although the ion chamber wandered badly.

It is seen that this monitor discriminates very sharply against low-energy background. It is believed that it will be very useful for monitoring the synchrotron beam for experiments in which relative beam monitoring is adequate and where the region of interest is the upper end of the bremsstrahlung spectrum. Several extensions of this monitoring technique are under consideration by the author and his colleagues. A variation that may make it possible to use this device for monitoring inside the bremsstrahlung spectrum has been suggested by Dr. R. Sagane.<sup>40</sup>



MU-6969

Fig. 11  
Schematic diagram of the magnetic monitor.

## V. RESULTS AND CONCLUSIONS

### A. Data

A total of 1,500,000 coincidence counts were taken in the course of three independent runs over the period of a year. The results were consistent within statistics.

In each run the three targets were cycled frequently, a one-hour cycle period being typical. As it was ratios of counting rate with dummy in to counting rate with absorber in that were to be measured, cycling would tend to cancel out long-time nonperiodic beam variations. In this same respect, every effort was made to minimize the number of trips into the magnet room in order to maintain machine stability.

Because the absorbers attenuated the beam by a factor of  $1/e$  at 300 Mev, the flux through the pair spectrometer in the desired energy interval would vary over a factor of almost three on switching from absorber to dummy. In order to assure that the spectrometer was always operating at the same efficiency, the synchrotron beam was varied so that the flux through the spectrometer was maintained at a constant value. Placing a portable Zeus meter behind the pair spectrometer helped the operator maintain this constant value.

### B. Cross Sections

The total absorption cross sections at 300 Mev in hydrogen and carbon were found to be  $(1.88 \pm 0.10) \times 10^{-26}$  cm<sup>2</sup>/hydrogen atom and  $(32.02 \pm 0.15) \times 10^{-26}$  cm<sup>2</sup>/C atom respectively. The errors listed are root-mean-square errors on counting statistics. The temperature of the targets was monitored and the data were corrected for density variation and change in target length. Over all, this correction amounted to less than 0.1%. The accidentals were subtracted from the total counts; and they amounted to less than 0.5%.

The calculations of the experimental triplet cross sections in hydrogen and carbon at 300 Mev are summarized in Table II below, and the theoretical cross sections are given for comparison.

Table II

Interaction	Hydrogen Cross Section (cm <sup>2</sup> )	Error	Carbon Cross Section (cm <sup>2</sup> )	Error
Nuclear Pair	0.768x10 <sup>-26</sup>	-	24.95x10 <sup>-26</sup>	-
Electron Compton	0.321	not greater than 10%	1.93	not greater than 10%
Photomeson	0.045	50%	0.28	factor of 2
Photostar	-	-	0.15	50%
Nuclear Photoeffect	-	-	0.01	factor of 10
Total (less triplet)	(1.134±0.039)x10 <sup>-26</sup>		(27.32±0.61)x10 <sup>-26</sup>	
Experimental Total Absorption Cross Sections	(1.88 ±0.10) x10 <sup>-26</sup>		(32.02±0.15)x10 <sup>-26</sup>	
Experimental Triplet Cross Sections	(0.75±0.11)x10 <sup>-26</sup>		( 4.70±0.62)x10 <sup>-26</sup>	
Theoretical Triplet Cross Sections	0.786x10 <sup>-26</sup>		4.511x10 <sup>-26</sup>	



It is to be noted that, with the exception of nuclear pair production, pair production in the field of the orbital electrons, and Compton effect, all other absorption processes in carbon contribute but 1.5% of the total absorption cross section. This amounts to 10% of the total triplet cross section in carbon, and when the uncertainties in some of these other cross sections are reduced the data are available in this experiment for the calculation of a better value for the triplet cross section in carbon.

#### ACKNOWLEDGMENTS

The author wishes to express his gratitude to Professor E. M. McMillan for his advice and encouragement throughout the course of this work.

It would be difficult to adequately thank my co-workers, Dr. R. W. Kenney and Mr. John Anderson, who have given their moral as well as physical support to this experiment. The author is indebted to Dr. R. F. Post for having suggested the experiment as well as having assisted in its early phases.

To Mr. George McFarland and the synchrotron crew go my appreciation and thanks for their efficient handling of the machine.

This work was done under the auspices of the Atomic Energy Commission.

REFERENCES

1. F. Perrin, *Compt. Rend.* 197, 110 (1933).
2. L. Landau and G. Rumer, *Proc. Roy. Soc. (London)* A166, 213 (1938).
3. J. A. Wheeler and W. E. Lamb, *Phys. Rev.* 55, 858 (1939).
4. A. Borsellino, *Helv. Phys. Acta.* 20, 136 (1947).  
*Nuovo cimento IV*, N3-4 (1947).
5. W. E. Ogle and P. G. Kruger, *Phys. Rev.* 65, 61 (1944).
6. K. M. Watson, *Phys. Rev.* 72, 1060 (1947).
7. V. Vortruba, *Phys. Rev.* 73, 1468 (1948).
8. J. A. Phillips and P. G. Kruger, *Phys. Rev.* 72, 164 (1947);  
*Phys. Rev.* 76, 1471 (1949).
9. E. R. Gaerttner and M. L. Yeater, *Phys. Rev.* 78, 621 (1950).
10. C. R. Emigh, *Phys. Rev.* 86, 1028 (1952).
11. J. W. DeWire, *Phys. Rev.* 82, 447 (1951).
12. J. L. Lawson, *Phys. Rev.* 75, 433 (1949).
13. A. I. Berman, *Phys. Rev.* 90, 211 (1953).
14. H. Bethe and W. Heitler, *Proc. Roy. Soc. (London)* A146, 83 (1934).
15. J. W. DeWire, A. Ashkin, and L. A. Beach, *Phys. Rev.* 83, 505 (1951).
16. L. C. Maximon and H. A. Bethe, *Phys. Rev.* 87, 156 (1952);  
H. A. Bethe and L. C. Maximon, *Phys. Rev.* 93, 768 (1954).
17. H. Davies, H. A. Bethe, and L. C. Maximon, *Phys. Rev.* 93, 788 (1954).
18. L. I. Schiff, Quantum Mechanics (McGraw-Hill Book Co., New York, 1949), 271.
19. W. Heitler, The Quantum Theory of Radiation (Oxford University Press, London, 1944) 271.
20. H. A. Bethe and A. Ashkin, Experimental Nuclear Physics, Vol. I, Pt. II (John Wiley and Sons Inc., New York, 1953), 263.
21. O. Klein and Y. Nishina, *Z. Physik* 52, 853 (1929).
22. R. W. Kenney, J. Dudley and C. McDonald, Jr., *Phys. Rev.* 93, 951(A) (1954).

23. F. Coensgen, The Electron Compton Effect at 250 Mev, University of California Radiation Laboratory Report No. UCRL-2413, November, 1953. Phys. Rev. 93, 948(A) (1954).
24. N. Jarmie, G. Repp, and R. S. White, Phys. Rev. 91, 1023 (1953).
25. Unpublished data from The California Institute of Technology.
26. R. Walker, D. Oakley, and A. Tollestrup, Phys. Rev. 89, 1301 (1953).
27. M. Jakobson, A. Shultz, and R. S. White, Phys. Rev. 91, 695 (1953).
28. J. Carothers, On the Ratio of  $\pi^+$  to  $\pi^-$ -Mesons Produced by Gamma Rays, University of California Radiation Report No. UCRL-1829, June 1952.
29. J. Steinberger, W. Panofsky, and J. Steller, Phys. Rev. 78, 802 (1950).
30. R. D. Miller, Phys. Rev. 82, 260 (1951).
31. L. Jones, UCRL-1916.
32. C. Levinthal and A. Silverman, Phys. Rev. 82, 822 (1951).
33. G. Chew and M. Goldberger, Phys. Rev. 77, 470 (1950).
34. J. C. Keck, Phys. Rev. 85, 410 (1952).
35. W. Heitler, The Quantum Theory of Radiation (Oxford University Press, London, 1944), 125.
36. H. A. Bethe and A. Ashkin, Experimental Nuclear Physics, Vol. I, Pt. II, (John Wiley and Sons Inc., New York, 1953), 316.
37. R. W. Keaney, Absolute Photon Attenuation Cross Section for Nonpair Processes in Beryllium at 300 Mev, University of California Radiation Laboratory Report No. UCRL-1654, February 1952.
38. L. Neher, Meson Production by High-Energy Neutrons, University of California Radiation Laboratory Report No. UCRL-2191, April, 1953.
39. C. McDonald, Jr., R. Kenney, and R. Post, Phys. Rev. 93, 951(A) (1954).
40. R. Sagane, Private Communication.
41. A. Bishop, The Photoproduction of Mesons from Hydrogen, University of California Radiation Laboratory Report No. UCRL-874, 12, August, 1950.
- W. Gilbert, Deuteron Photodisintegration at High Energies, University of California Radiation Laboratory Report No. UCRL-1590, 31, December, 1951.